Supporting Materials – Rosenblad & Ackerly (2026) "Ecological lines of least resistance shape community responses to climate change"

Appendix S1 – additional methodological details

Tree census data preparation

We filtered the FIA tree census data to only include plots with a 10-year interval between censuses. (Due to delays in census implementation, 579 plots had inter-census intervals that were not exactly 10 years, so this filtering step reduced the dataset from 11,858 forest plots to 11,279.) Following Rosenblad et al. (2023), we excluded plots at which FIA field crews noted biomass harvesting, or any other type of anthropogenic disturbance or artificial recruitment. In estimating the effect of θ on community-climate disequilibrium, we also excluded plots that contained only one species at baseline, as these plots exhibited no variation in species' niche optima, and thus the major axis of niche variation required to compute θ was not defined.

Below, we discuss an alternate version of the data set that was analyzed in a sensitivity analysis.

Alternate tree census dataset

In an alternative analysis, we used an updated version of the FIA dataset, which includes census data through 2024, but which requires additional filtering. This is because in some regions of our western US study domain, FIA field crews extend the census plot boundaries beyond the nationally standardized plot design for trees above a certain size. Thus, if we do not include a data filtering step to remove these additional trees, then FIA plots censused under these nonstandard protocols are not comparable to plots censused under the nationally standardized protocol. When the Rosenblad et al. (2023) dataset was analyzed, the publicly available FIA dataset included the location of each tree within each plot, which allowed Rosenblad et al. (2023) to re-standardize nonstandard plot data by excluding any tree recorded beyond the standard boundaries. Shortly after Rosenblad et al. (2023) was published, the FIA program ceased publishing individual tree location data. Consequently, to achieve spatiotemporal consistency of census methods in the updated FIA dataset, we had to exclude any plot that was censused according to a nonstandard protocol. This yielded a data set of 7,657 plots with censuses spanning 2000 to 2024.

Inferring species' climatic niche optima

We estimated each species' climatic niche optimum for all four climate variables (TMAX, TMIN, AET, and CWD) using a presence-absence climatic niche model fit to the FIA data from the baseline round of tree censuses. The inferred niche optimum is the value of each climate variable with the greatest estimated probability of occurrence, after marginalizing predicted occurrence probabilities over the other climate variables. This approach is designed to estimate the optimal value of each climate variable while controlling for the other variables, which might otherwise confound our estimates (Arif & MacNeil 2023).

We generated each species' presence-absence data set by circumscribing a minimum convex polygon in geographic space around all plots where the focal species was observed. This polygon is expanded by a 100 km buffer, within which all plots (both presences and absences) are selected. (Some species' ranges extend beyond the western US, and we did not include these portions of their ranges.)

Our models were built using the mgcv R package (Wood 2011), with a one-dimensional thin plate regression spline for each climate variable. We accounted for spatial non-independence by using an isotropic two-dimensional spline over plots' geographic coordinates.

Hypothesis test – alternate analyses

Our main model used an identity link function and a Student's t error distribution, which we estimated using mgcv (Wood 2011). The linear predictor included a linear term for θ, a linear term for the magnitude of climate change, a linear term for the initial community-climate disequilibrium, a linear term for "axis dominance", and a two-dimensional, isotropic smoothing spline over plots' spatial coordinates. (Axis dominance represents the proportion of total variation in niche optima explained by the line of least resistance.) Axis dominance and initial disequilibrium also had interaction terms with θ. The spatial smooth term used the mgcv R package's thin plate regression spline with a basis dimension of 10. Models were fit via restricted maximum likelihood.

The model structure was the same in all alternative analyses, with the following exceptions. In the analysis that used one-dimensional disequilibrium in TMIN as the response variable, a basis dimension of 20 was necessary for the spatial smoothing spline to account for residual spatial autocorrelation. The AET model required a basis dimension of 15. In the analysis that only used TMIN and AET to compute both θ and community-climate disequilibrium, a basis dimension of 15 was needed. The model for TMIN and CWD required a basis dimension of 20. In the analysis of the updated FIA tree census data, which required more extensive data filtering, the necessary basis dimension was 15.

Confirming ecological relevance of climate variables

We used a null model permutation test to estimate the distribution of effect sizes we would expect in our main analysis if species' abundances were changing randomly over time, with no influence of climate. We reasoned that if our chosen climate variables affect species' demographic performance, then we should observe a weaker effect of θ on community-climate disequilibrium when the observed changes in species abundance are replaced by random changes. We simulated this scenario by reshuffling the observed plot-level species abundance growth rates. We used this procedure to produce 1,000 "null" datasets. For each null dataset, we re-fit the generalized additive model structure used in our main analysis. We then compared our observed effect size estimate to its null distribution. If the observed effect size is extreme relative to the null, we interpret this as evidence that our chosen climate variables are ecologically relevant. We also repeated this procedure for each of the six analyses examining each possible pairing of climate variables.

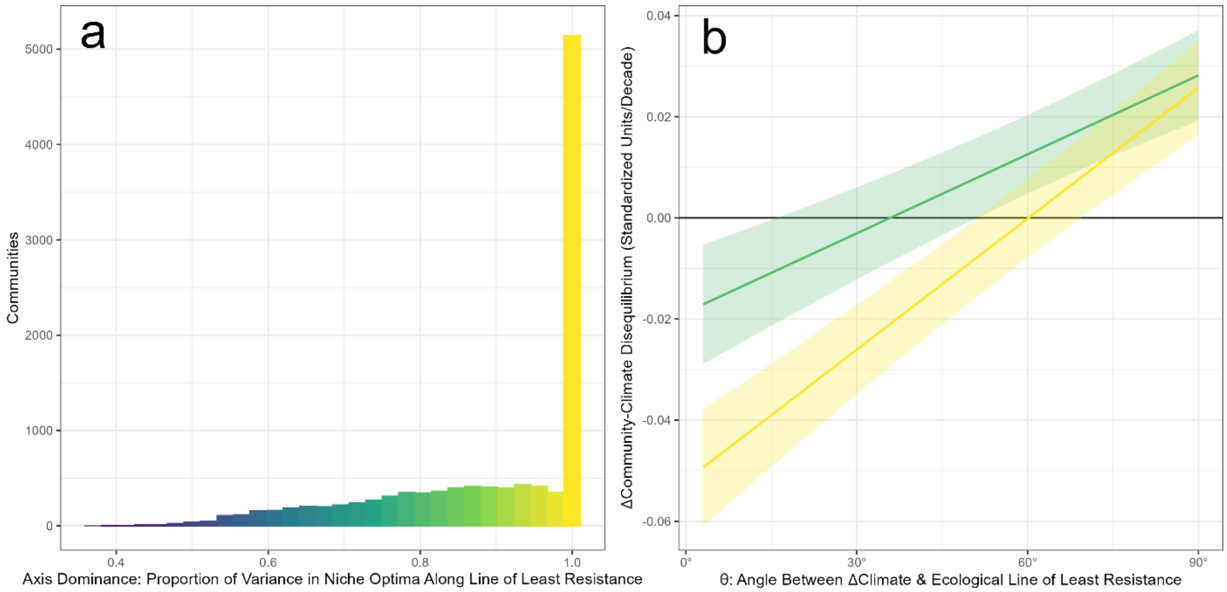

Fig. S1: a) *Observed distribution of "axis dominance"—the proportion of total variance in niche optima explained by the ecological line of least resistance. Greater axis dominance indicates stronger clustering of niche optima around the line of least resistance. The spike at 1.0 is due to communities with only two tree species.* **b)** *Axis dominance modifies the effect of θ on community-climate disequilibrium. The effect of θ is shown at two levels of axis dominance, the 25^{th} and 75^{th} percentiles.*

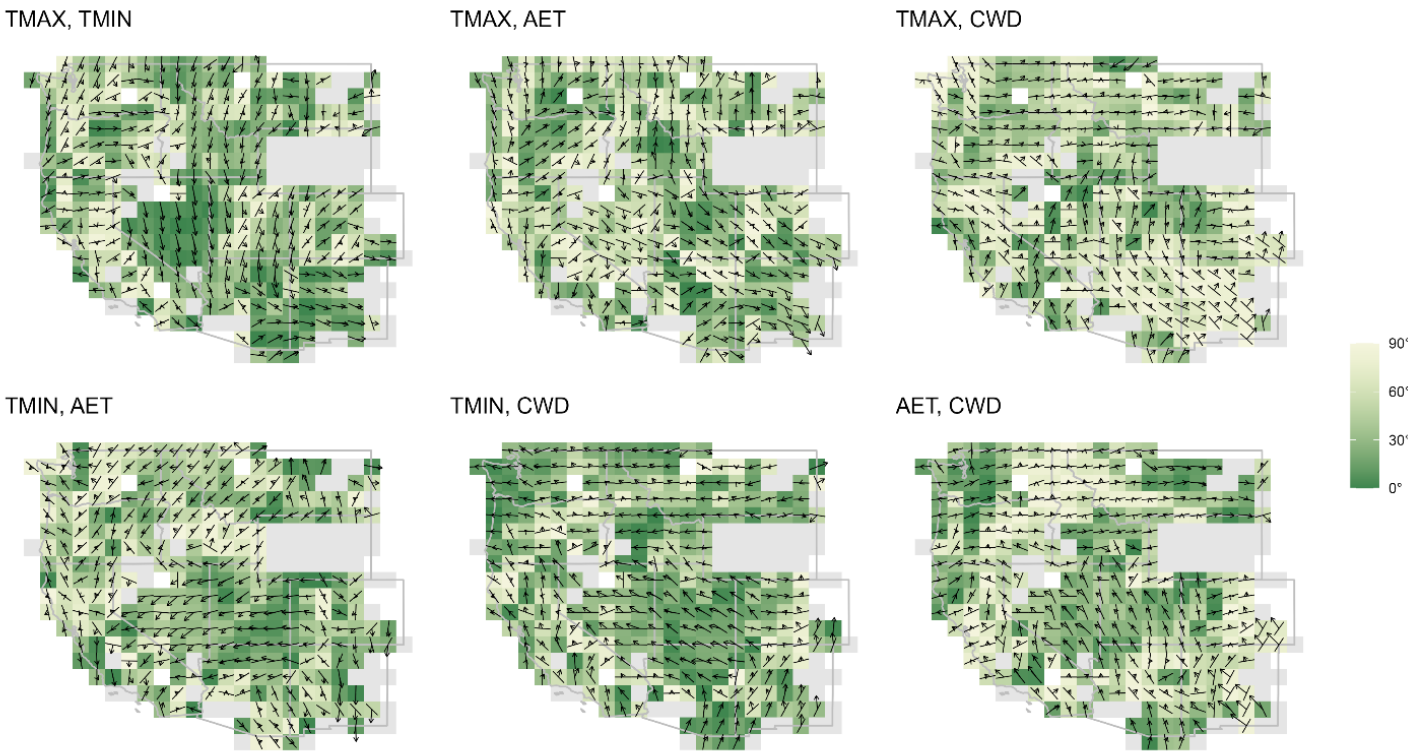

Fig. S2: G*eographic variation in θ for all pairs of climate variables. Climate and tree census data from the initial round of censuses are pooled within one-degree latitude/longitude map grid cells. Each grid cell shows a two-dimensional climate space. (White cells contain no tree census plots in our data set. Gray cells contain plots not visited during the baseline round of censuses.)*

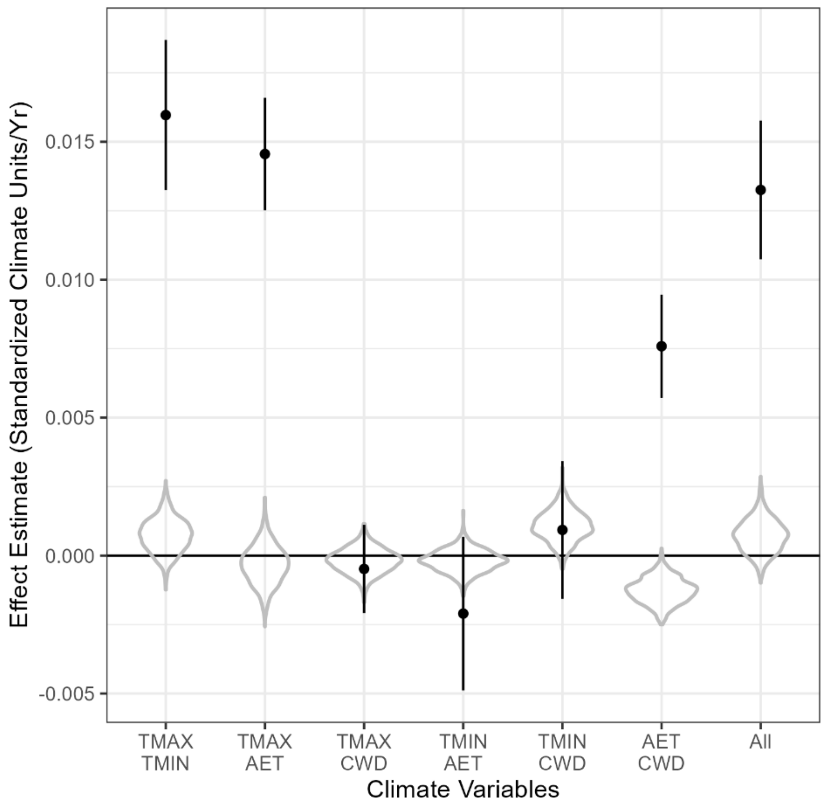

Fig. S3: *Results from null model tests of each climate variable's ecological relevance. Black dots represent the effect of θ on community-climate disequilibrium estimated from the observed data, and accompanying black whiskers represent 95% confidence intervals. Gray violins represent estimated null distributions of these effect sizes in a scenario of random species abundance change over time.*

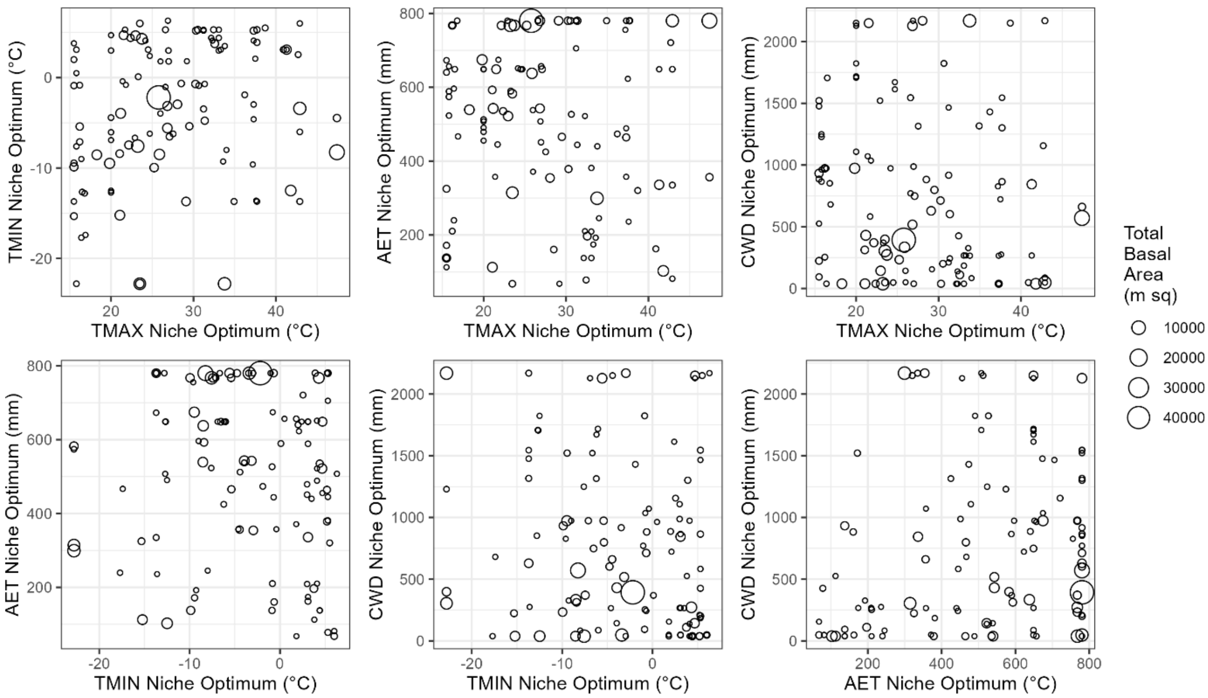

Fig. S4: *Bivariate relationships between species' inferred niche optima for four climate variables: TMAX (mean daily maximum temperature of the warmest month), TMIN (mean daily minimum temperature of the coldest month), AET (actual evapotranspiration), and CWD (climatic water deficit). Points represent species. Point size represents the total basal area of all individuals in the baseline round of tree censuses. Niche optima were inferred from the initial round of tree census data using generalized additive models.*

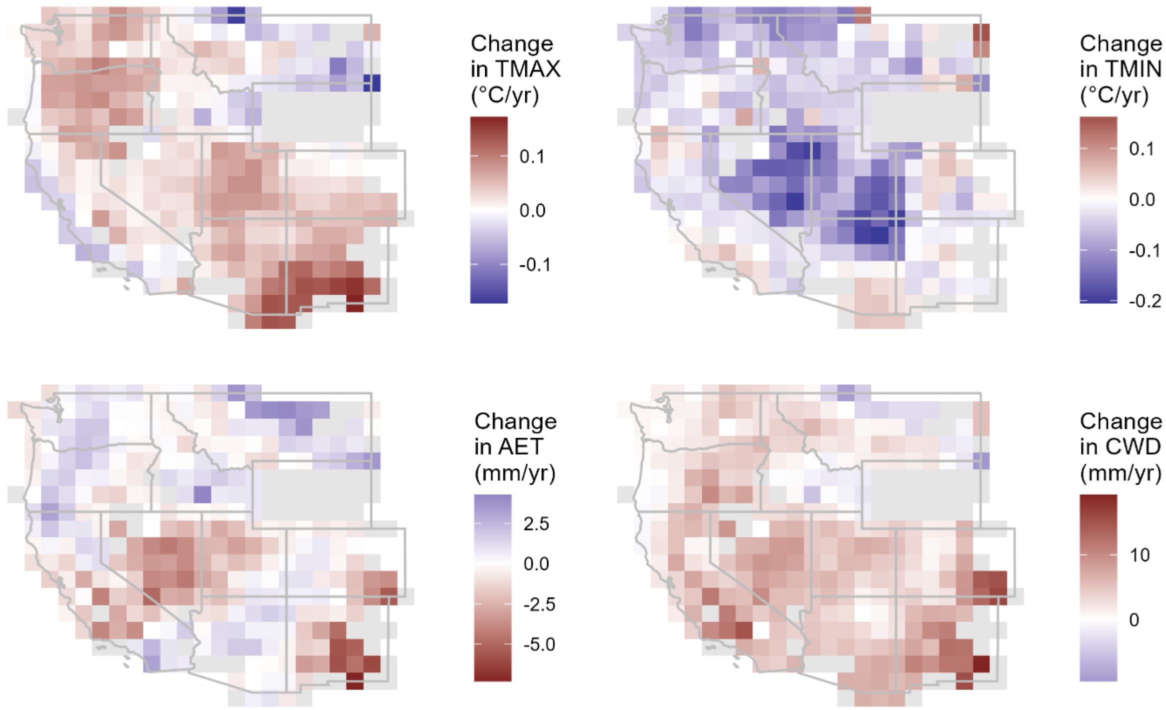

Fig. S5: *Mean rates of climate change across western US forest plots during the 10-year interval between forest censuses. Values were averaged among forest plots within each map grid cell.*

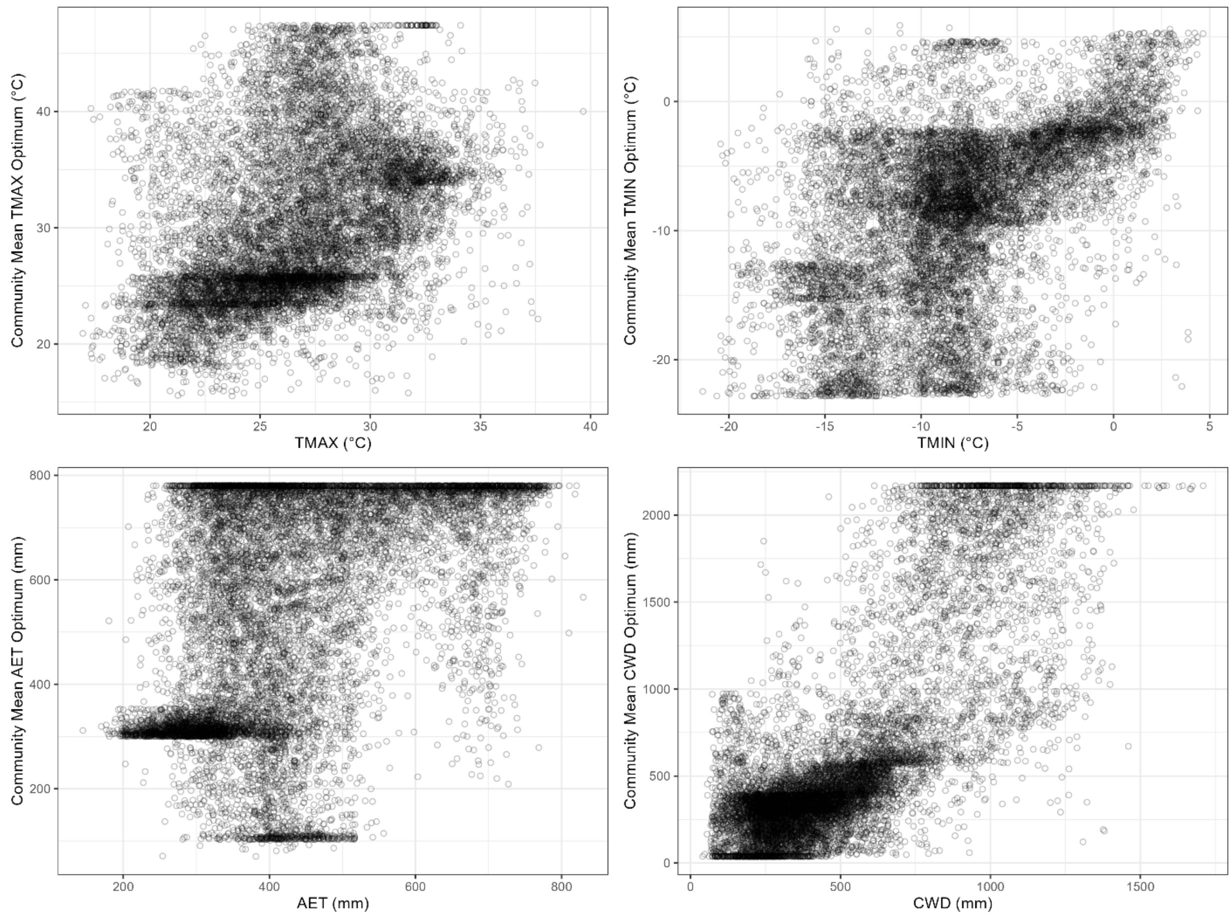

Fig. S6: *Bivariate relationships between climate variables and corresponding community mean niche optima at the baseline round of tree censuses.*

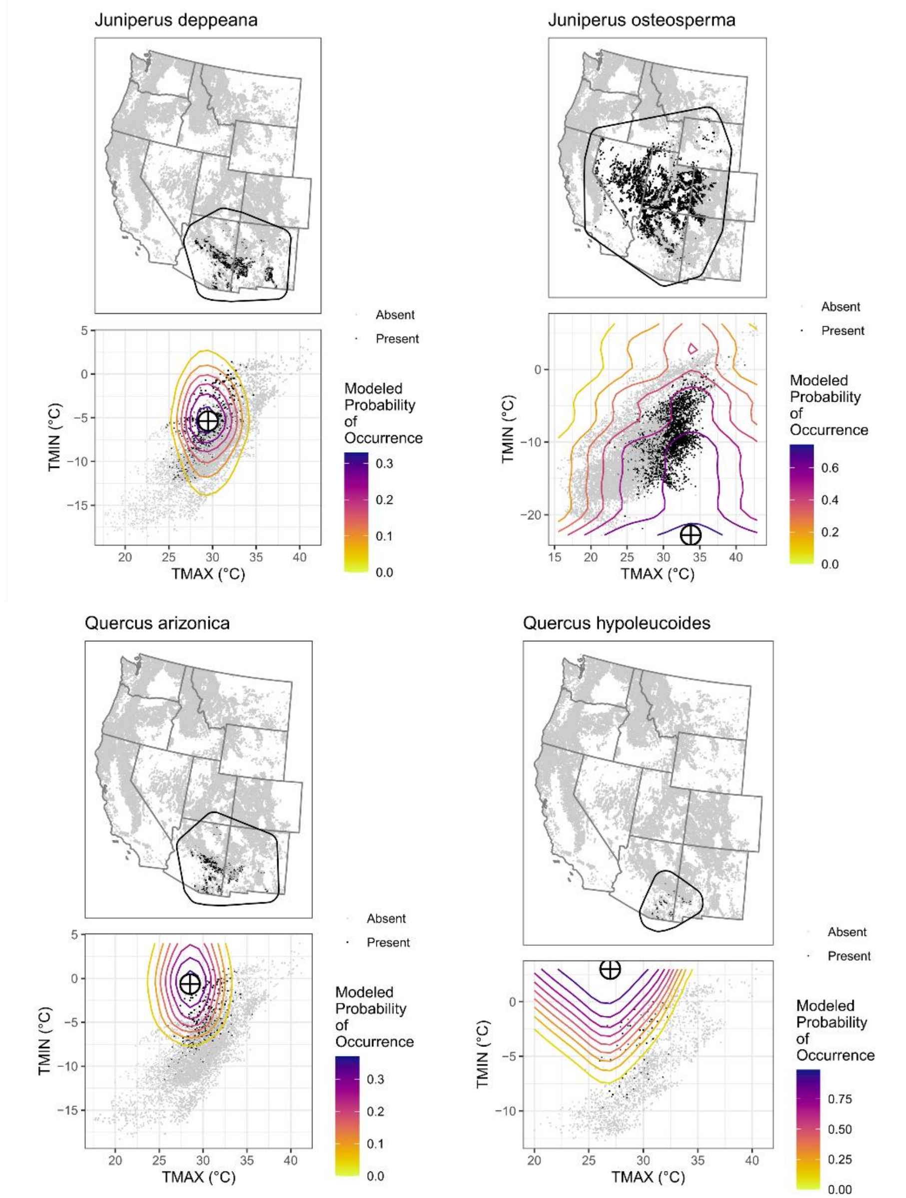

Fig. S7: *Geographic distributions and climatic niche plots, analogous to Fig. 2a-b, for the other species in the example communities shown in Fig. 2c-d.*

Predictor	Standardized Effect Estimate	95% Confidence Interval
θ	0.013	0.011, 0.016
Magnitude of Climate Change	0.011	0.0086, 0.014
Initial Community-Climate Disequilibrium	-0.024	-0.027, -0.021
Axis Dominance	-0.0093	-0.012, -0.0066
θ * Magnitude of Climate Change	0.014	0.012, 0.017
θ * Axis Dominance	0.0049	0.0023, 0.0074

Table S1: Summary of standarized effect estimates for predictor variables in the main regression analysis, a generalized additive model with a Student's t error distribution. The response variable is the observed temporal change in the distance between the climate and the community mean climatic niche optimum, as measured in multivariate climate space. Standardized effect size estimates show the effect on the response variable of increasing each predictor by one standard deviation.

Variable	Mean	Standard Deviation
Baseline TMAX (°C)	26.7	3.63
Baseline TMIN (°C)	-7.97	4.77
Baseline AET (mm)	434	133
Baseline CWD (mm)	527	303
ΔTMAX (°C/decade)	0.357	0.477
ΔTMIN (°C/decade)	-0.734	0.605
ΔAET (mm/decade)	-5.13	20.4
ΔCWD (mm/decade)	7.90	26.5
Baseline Community TMAX Niche Optimum (°C)	30.5	6.94
Baseline Community TMIN Niche Optimum (°C)	-8.63	6.76
Baseline Community AET Niche Optimum (mm)	542	212
Baseline Community CWD Niche Optimum (mm)	659	614
ΔCommunity TMAX Niche Optimum (°C/decade)	0.0249	2.04
ΔCommunity TMIN Niche Optimum (°C/decade)	0.223	2.00
ΔCommunity AET Niche Optimum (mm/decade)	4.12	46.9
ΔCommunity CWD Niche Optimum (mm/decade)	0.900	88.1
θ (°)	59.4	19.8
ΔCommunity-Climate Disequilibrium (standardized units/decade)	0.00776	0.252

Table S2: *Summary statistics for plot-level variables. Community-climate disequilibrium reflects distance in a four-dimensional climate space, where each climate variable has been standardized by its mean and standard deviation.*

Niche Optimum	Mean	Standard Deviation
TMAX	27.5	8.45
TMIN	-3.35	7.56
AET	509	224
CWD	771	676

Table S3: *Summary statistics for species' inferred climatic niche optima.*

	TMAX	TMIN	AET	CWD
TMAX	1	0.24	-0.067	-0.19
TMIN	0.24	1	-0.078	-0.18
AET	-0.067	-0.078	1	0.25
CWD	-0.19	-0.18	0.25	1

Table S4: *Unweighted correlation matrix for species' climatic niche optima across four climate variables: TMAX (mean daily maximum temperature of the warmest month), TMIN (mean daily minimum temperature of the coldest month), AET (actual evapotranspiration), and CWD (climatic water deficit).*

	TMAX	TMIN	AET	CWD
TMAX	1	-0.070	0.015	0.059
TMIN	-0.070	1	0.48	-0.26
AET	0.015	0.48	1	-0.2
CWD	0.059	-0.26	-0.2	1

Table S5: *Abundance-weighted correlation matrix for species' climatic niche optima across four climate variables: TMAX (mean daily maximum temperature of the warmest month), TMIN (mean daily minimum temperature of the coldest month), AET (actual evapotranspiration), and CWD (climatic water deficit). The weight for each species is its summed basal area across all plots in the baseline round of tree censuses.*